Supplementary Information for

Direct nitration and azidation of aliphatic carbons by an iron-dependent halogenase

Megan L Matthews, Wei-chen Chang, Andrew P Layne, Linde A Miles, Carsten Krebs, J Martin Bollinger Jr

SUPPLEMENTARY RESULTS

Supplementary Table 1. Parameters derived from titrations monitoring binding of anions to the SyrB2•Fe(II)•αKG and SyrB2-A118G•Fe(II)•αKG complexes. K_D values were determined by plotting ΔAbs at the wavelength of maximum change versus [Y^-] and applying a hyperbolic or quadratic fit, as appropriate for the weak- and tight-binding regimes, respectively (See ***Supplementary Figs. 4, 5, 10, 11***).

Anion	Formula	K_D (mM) WT SyrB2	λ (nm)	Number of Trials[b]	K_D (mM) A118G	λ (nm)	Number of Trials[b]
chloride	Cl^-	0.05 ± 0.025	530	6	43 ± 15	530	3
cyanide	CN^-	0.14 ± 0.05	515	2	*c*	*c*	3
sulfide	HS^-	0.47 ± 0.012	540	3	*a*	*a*	3
cyanate	OCN^-	0.2 ± 0.14	540	2	0.030 ± 0.015	540	3
azide	N_3^-	0.12 ± 0.005	545	2	0.15 ± 0.03	540	3
bromide	Br^-	0.47 ± 0.15	525	3	20 ± 7	520	2
formate	HCO_2^-	~ 3	530	1	*a*	*a*	1
nitrite	NO_2^-	~ 0.072	460	1	*c*	*c*	1
thiocyanate	SCN^-	*a*	*a*	2	0.34 ± 0.18	515	2

[a] No evidence for binding.

[b] In some trials, the [αKG] was 1.5 mM rather than 5 mM. This difference had no effect on the anion affinity.

[c] Titration spectra were anomalous as a consequence of features either inherent to the anion (NO_2^-) or that developed upon interaction with components in the solution [likely between the anion and free Fe(II) ions].

Supplementary Table 2. Comparison of Mössbauer parameters of quadrupole doublets associated with Fe(IV) complexes formed in SyrB2 in the presence of various substrates and anions.

Substrate	Anion/Enzyme	Total Fe(IV)	δ_1 (mm/s)	$\Delta E_{Q,1}$ (mm/s)	δ_2 (mm/s)	$\Delta E_{Q,2}$ (mm/s)	$\Gamma_{1,2}$ (mm/s)	Fraction $Fe(IV)_1$:$Fe(IV)_2$
Thr-*S*-SyrB1[a]	Cl^-/SyrB2	-	0.30	1.09	0.23	0.76	0.22	4:1
Thr-*S*-SyrB1	N_3^-/SyrB2	0.78	-	-	0.20	0.77	0.40	-
d_5-Thr-*S*-SyrB1	HS^-/SyrB2	0.43	-	-	0.25	1.14	0.23	-
d_5-Thr-*S*-SyrB1	CN^-/SyrB2	0.41	-	-	0.22	0.99	0.40	-
d_5-Thr-*S*-SyrB1	NO_2^-/SyrB2	0.37	-	-	0.32	1.20	0.25	-
d_5-Nva-*S*-SyrB1	Cl^-/SyrB2	0.49	0.25	1.19	0.23	0.74	0.27	0.33:0.66

[a] ref. [1]

Supplementary Table 3. Comparison of Mössbauer parameters of quadrupole doublets associated with the Fe(II) starting complexes formed in SyrB2 in the presence of various substrates and anions.

Substrate	Anion/Enzyme	δ_1 (mm/s)	$\Delta E_{Q,1}$ (mm/s)	δ_2 (mm/s)	$\Delta E_{Q,2}$ (mm/s)	$\Gamma_{1,2}$ (mm/s)	Ratio $Fe(II)_1$:$Fe(II)_2$
Thr-*S*-SyrB1[a]	Cl^-/SyrB2	1.22	2.87	1.07	2.62	0.26	7:1
d_5-Thr-*S*-SyrB1	no Y^-/SyrB2	1.25	2.95	1.18	2.30	0.37	0.95:0.10
Thr-*S*-SyrB1	N_3^-/SyrB2	1.22	2.93	1.12	1.95	0.32	0.90:0.10
d_5-Thr-*S*-SyrB1	HS^-/SyrB2	1.17	3.15	1.03	2.79	0.26	0.72:0.28
d_5-Thr-*S*-SyrB1	CN^-/SyrB2	1.23	2.87	1.14	3.20	0.38	0.65:0.35
d_5-Thr-*S*-SyrB1	NO_2^-/SyrB2	1.15	2.35	1.32	2.95	0.40	0.86:0.14
d_5-Thr-*S*-SyrB1	Cl^-/SyrB2	1.27	2.77	1.06	2.51	0.27	0.40:0.60

[a] ref [1]

Supplementary Table 4. MS fragmentations corresponding to relevant parent ions and iminium daughter ions of Aba-derived substrates and products in the reaction with SyrB2.

Product	Parent m/z	Daughter m/z
L-glycine	76.1	30.1
Aba	104.1	58.1
3,3-d_2-Aba	106.1	60.1
4-N_3-Aba	145.1	99.1
3,3-d_2-4-N_3-Aba	147.1	101.1
3,3-d_2-4-$^{15}NN_2$-Aba	148.1	102.1
4-NO_2-Aba	149.1	103.1
3,3-d_2-4-NO_2-Aba	151.1	105.1
3,3-d_2-4-$^{15}NO_2$-Aba	152.1	106.1

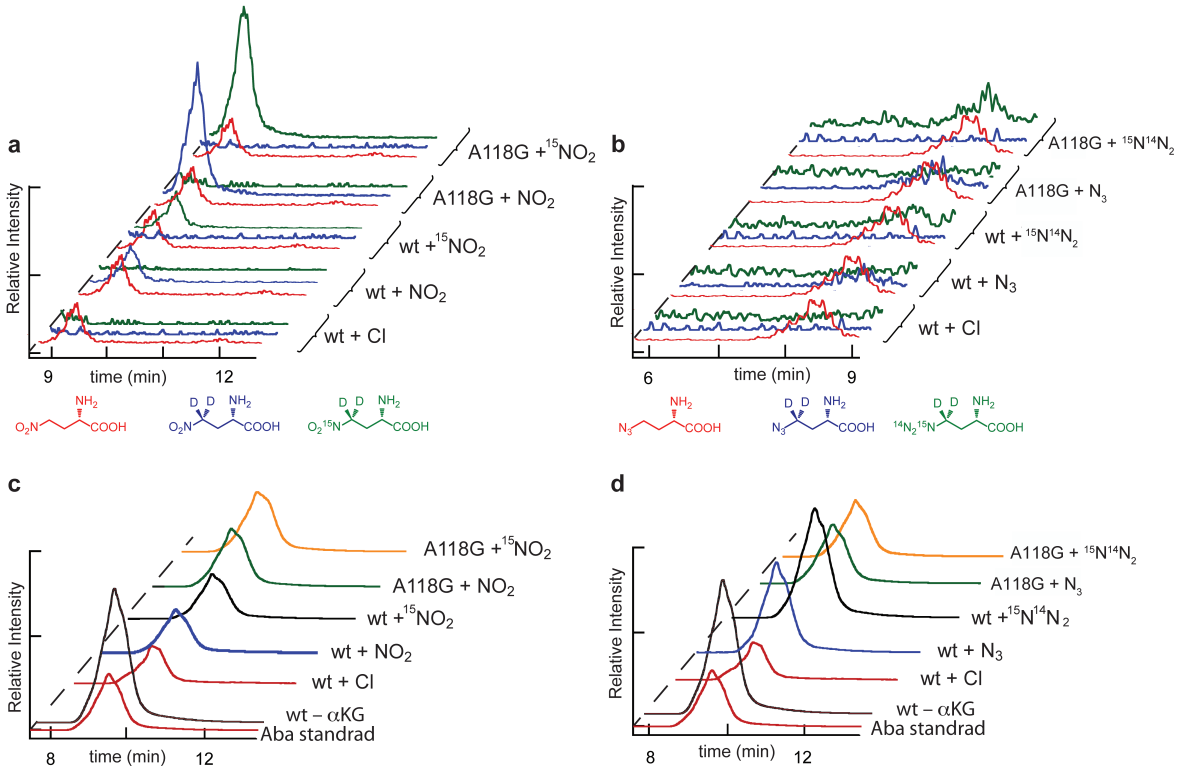

Supplementary Figure 1. LC-MS/MS chromatograms comparing yields of the C–N coupling products and substrate consumption in the reactions of the wild-type SyrB2 and A118G variant. Panel ***a*** illustrates detection of the nitration product and ***b*** the azidation product. Panels ***c*** and ***d*** illustrate the 3-d_2-Aba recovered after hydrolysis of the substrate in reactions of ***a*** and ***b***, respectively. For each reaction condition in ***a*** and ***b*** along the *z*-axis, defined by the enzyme (wild-type vs. A118G) and anion added, parent-to-daughter ion transitions (***Supplementary Table 4***) for the unlabeled nitrogenous product standard added to the reaction sample (*red*) and the authentic products formed from the 3-d_2-Aba-*S*-SyrB1 substrate with either natural abundance (*blue*) or isotopically enriched (+1) NO_2^- /N_3^- (*green*) anion were monitored. Only the transition for the standard is observed for reactions with the wild-type enzyme in the presence of Cl^- (*first condition along z-axis in* ***a*** *and* ***b***). In ***c*** and ***d***, the transition for 3-d_2-Aba is compared to that for both an unlabeled

Aba standard and 3-d_2-Aba recovered in the control reaction lacking αKG. The reactions were performed as described in ***Online Methods***, with the following exceptions. The final concentrations of the reactants were 0.25 mM Fe(II), 0.25 mM SyrB2, 0.325 mM αKG, 0.090 mM 3-d_2-Aba-*S*-SyrB1 and 1.25 mM NO_2^- (***a*** and ***c***) or N_3^- (***b*** and ***d***). The 3-d_2-Aba-*S*-SyrB1 substrate was assembled by incubation of 0.18 mM holo-SyrB1, 0.11 mM 3-d_2-Aba, 2.2 mM ATP, and 2.2 mM $MgSO_4$ for 30 min at ambient temperature and was used without desalting. Note that differences in the reaction conditions used here (specifically, greater αKG and N_3^- concentrations) with respect to those used in the experiment of ***Figure 5*** result in a lesser enhancement of azidation by the A118G variant relative to the wild-type enzyme and a greater enhancement of nitration. The figure depicts a single trial, which is one of several replicates.

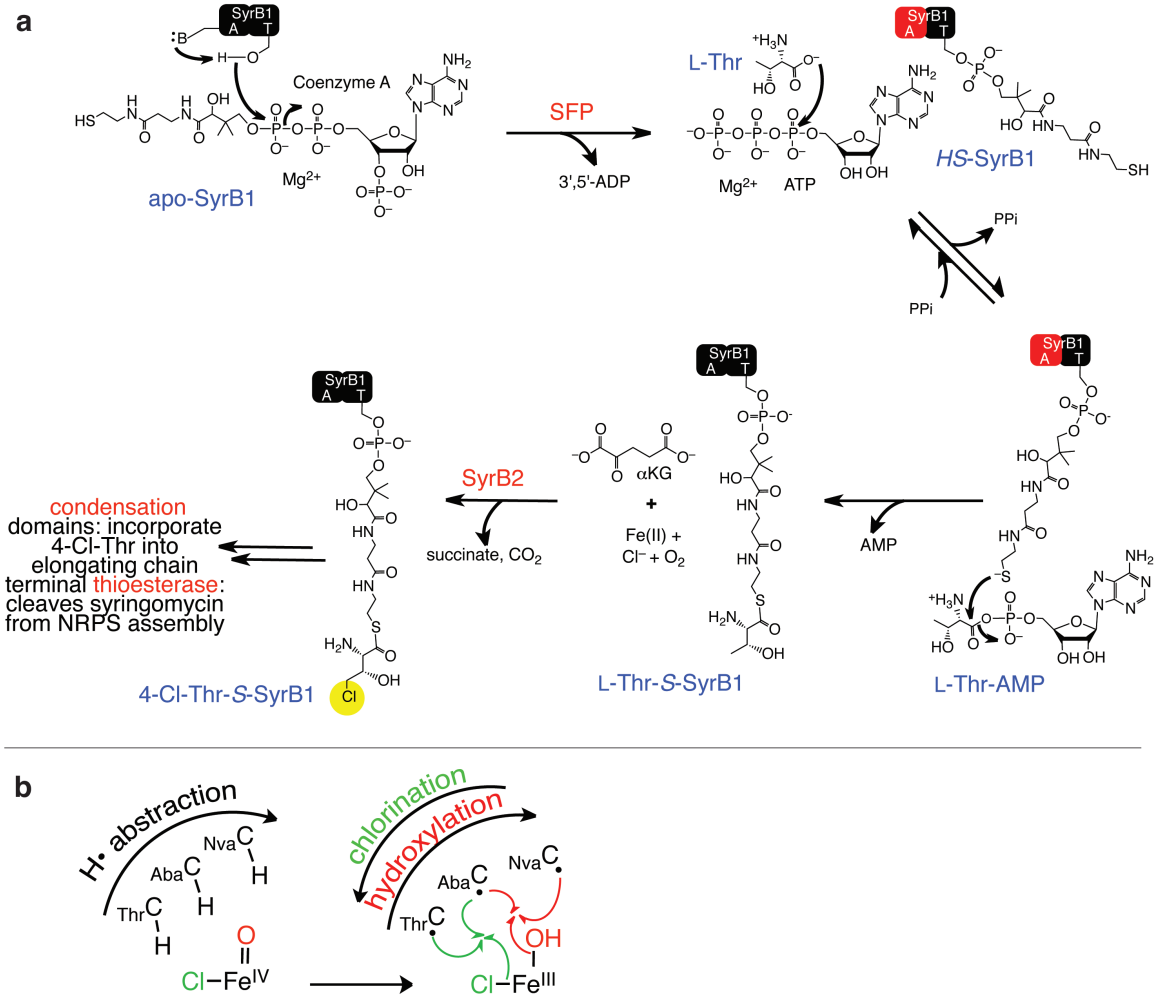

Supplementary Figure 2. (***a***) Assembly and chlorination of the native SyrB2 substrate, L-threonine appended to the phosphopantetheine cofactor of SyrB1 (abbreviated Thr-*S*-SyrB1). In the Syr halogenation system, the amino-acid-charging (adenylation) function and carrier protein are fused in a single polypeptide, SyrB1. (***b***) Enhanced hydrogen abstraction in Aba-*S*-SyrB1, and even more so in the L-norvalinyl-*S*-SyrB1 substrate, Nva-*S*-SyrB1, is correlated with enhanced hydroxylation[2].

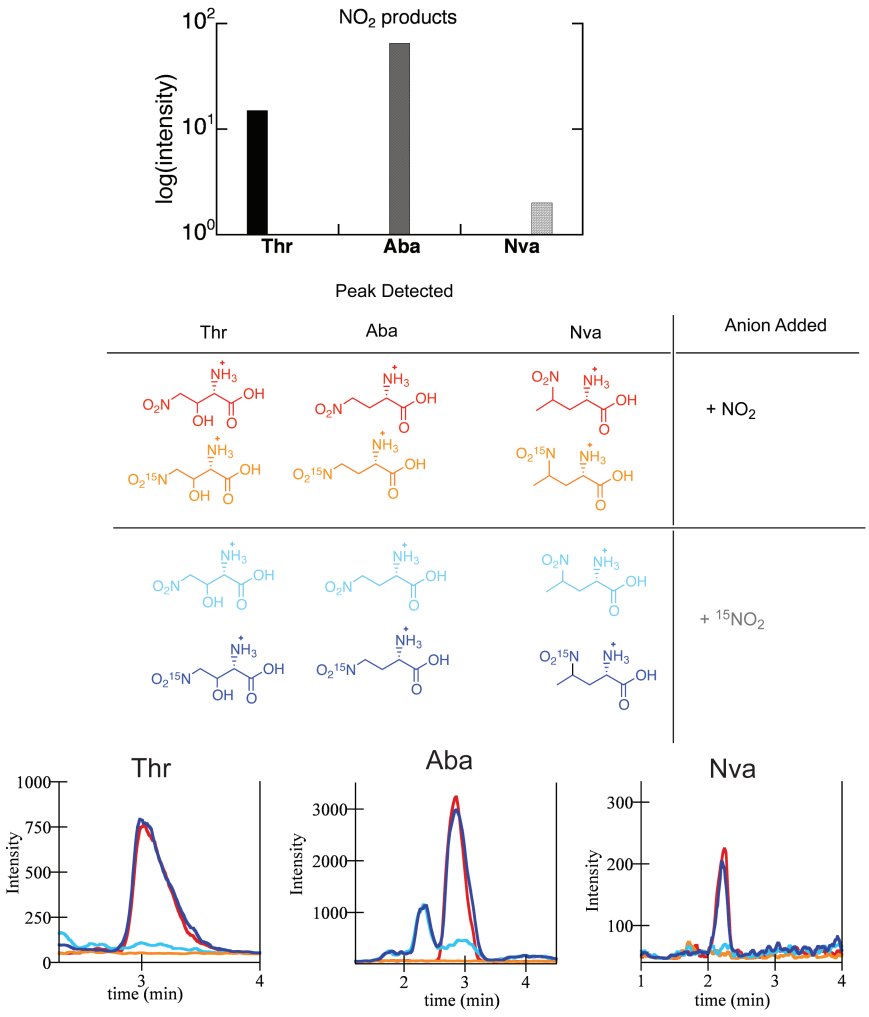

Supplementary Figure 3. Analysis of relative nitration yields in the reactions with the native, chlorination-predominant Thr-*S*-SyrB1 substrate, the ambivalent Aba-*S*-SyrB1 substrate, and the hydroxylation-predominant Nva-*S*-SyrB1 substrate. ***Top***: bar graph showing intensities of the peaks for the nitration products of the three substrates. ***Middle***: color key for the chromatograms at bottom. Note that the structure of the detected nitro-Nva product (specifically, the carbon to which the nitro group is attached) is not known but is assumed on the basis of published results[2]. ***Bottom***: LC-MS SIM chromatograms for the nitration products of the three substrates produced by SyrB2 in the presence of $^{14}NO_2^-$ or $^{15}NO_2^-$. The reactions were carried out with 0.6 mM of each reaction

component [SyrB2, Fe(II), αKG, aminoacyl-*S*-SyrB1 (Thr-*S*-SyrB1, Aba-*S*-SyrB1, or Nva-*S*-SyrB1), and $^{14}NO_2^-$ or $^{15}NO_2^-$]. Subsequent to initiation by addition of the Thr-*S*-SyrB1, Aba-*S*-SyrB1, or Nva-*S*-SyrB1 substrate, O_2-saturated reaction buffer was added to bring [O_2] to ~ 0.6 mM. L-glycine, an amino acid that SyrB1 cannot append to its carrier domain, was added as normalization standard to 0.6 mM. The products and the remaining SyrB1-appended d_2-Aba were released from the carrier protein by treatment with KOH (0.25 M). After a 1 min incubation at room temperature, an approximately equal volume of 1.5 % $HClO_4$ (in water) sufficient to achieve pH neutrality was added, and the neutral solution was stored at -20 ºC for 1 h to permit precipitation of $KClO_4$. Protein was removed from the samples by using a Microcon centrifugal filter unit (Millipore) with a 10-kDa molecular mass cut-off filter. The chromatography was performed as previously described[2], with the exception that the ZIC-HILIC column was developed isocratically at 0.3 mL/min with a 70%/30% acetonitrile/20 mM ammonium formate (pH 6) mobile phase. In each acquisition method, parent amino acid cations and iminium daughter ions produced from a neutral loss of CO_2 and H_2 (a combined mass of 46 atomic mass units) were selectively monitored (see ***Supplementary Table 4*** for MS fragmentations). The results are from a single trial.

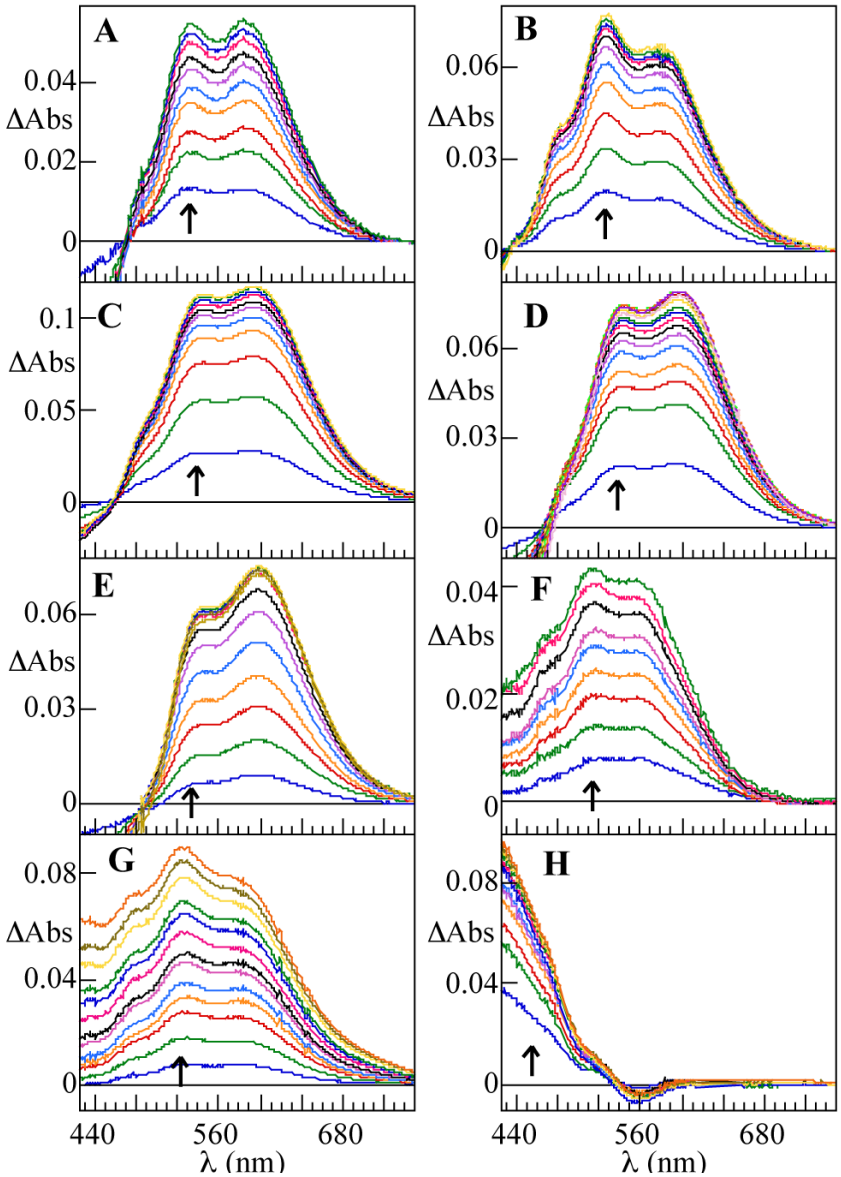

Supplementary Figure 4. Effect of anion binding on the MLCT absorption band during titration of (***a***) Cl^-, (***b***) Br^-, (***c***) N_3^-, (***d***) OCN^-, (***e***) HS^-, (***f***) CN^-, (***g***) HCO_2^-, or (***h***) NO_2^- into a solution of 0.75 mM Fe(II), 5 mM αKG, and 1 mM SyrB2. ***a***, ***c***, and ***h*** are duplicated from ***Figure 3*** in the main manuscript to facilitate comparison. The anion concentrations after each addition are shown as the x-axes in ***Supplementary Figure 5***. Each panel represents a single trial.

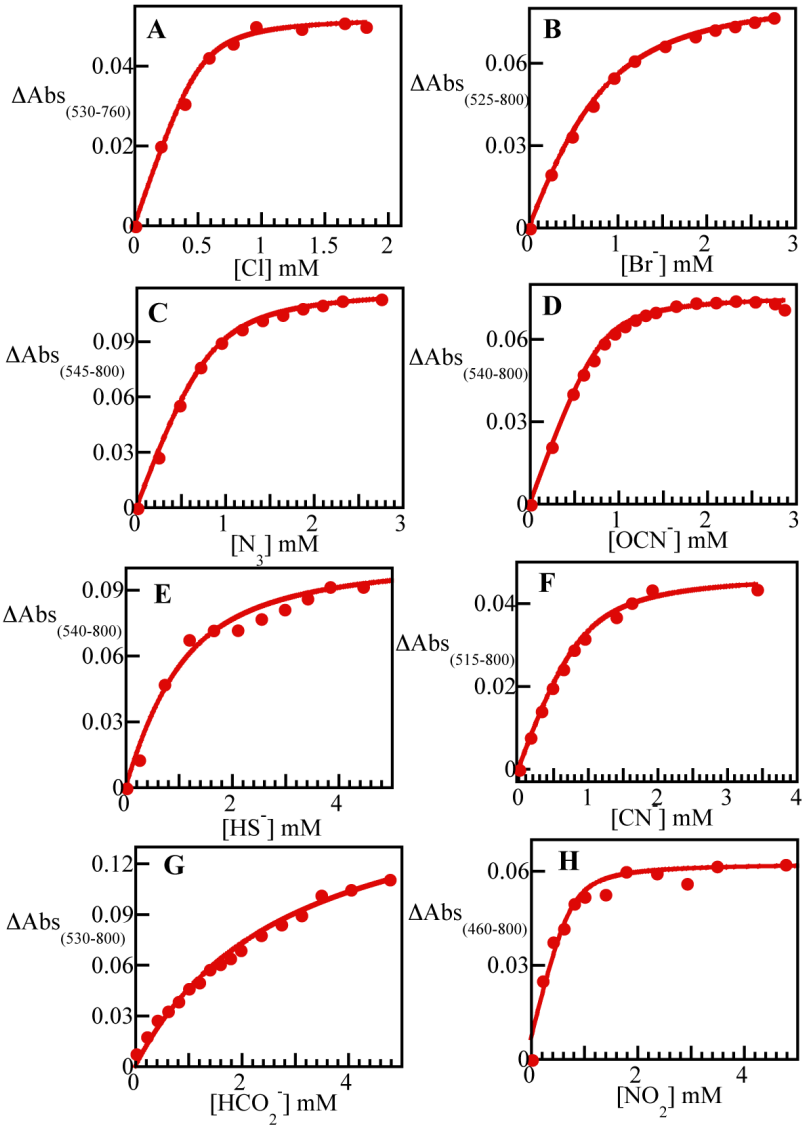

Supplementary Figure 5. Plots of the change in absorbance versus [Y^-] obtained from the titrations depicted in ***Supplementary Figure 4***. Anion K_D values (summarized in ***Supplementary Table 1***) were determined by fitting the data to a hyperbolic binding equation (if in the weak-binding regime, as in ***g*** and ***h***) or the quadratic binding equation (if in the tight-binding regime, as in ***a-f***). Each panel represents a single trial.

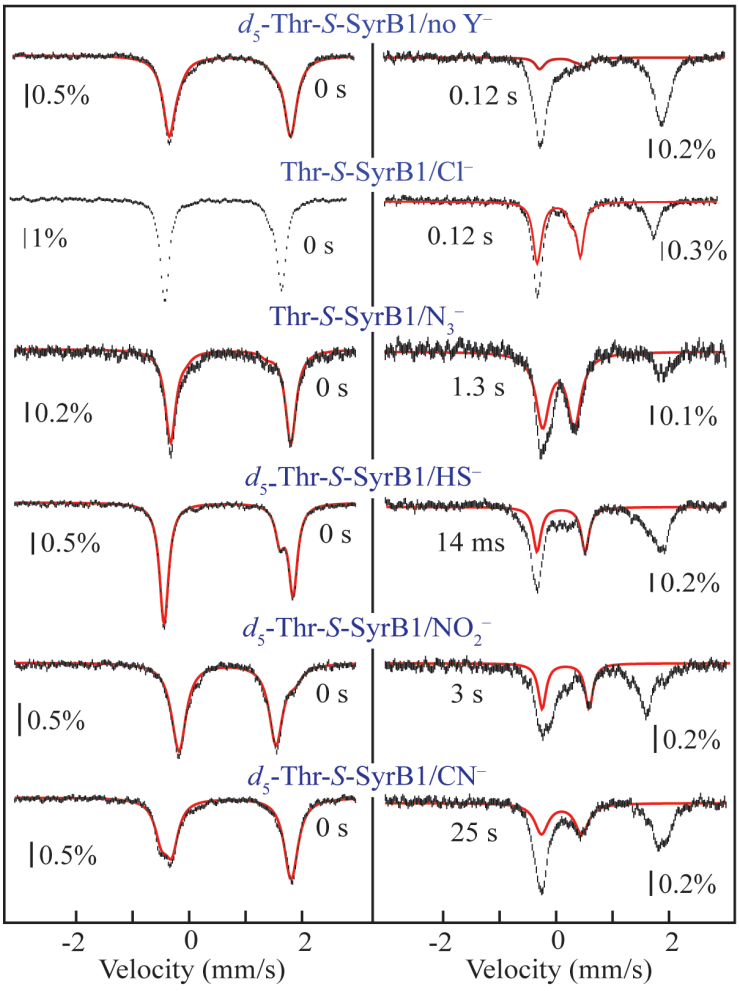

Supplementary Figure 6. Mössbauer spectra of selected samples prepared by reacting the SyrB2•Fe(II)•αKG•d_5-Thr-*S*-SyrB1 complex (unlabeled Thr-*S*-SyrB1 in the case of the reactions with $N_3^-$and Cl^-) in the presence of the indicated anion at 5 °C with O_2-saturated buffer. Reaction times are indicated. A doublet indicative of Fe(IV) is absent in the sample for which no anion was intentionally added. Solid lines (in red) are simulations of the summation of the Fe(II) components (*left panel*) or Fe(IV) component(s) (*right panel*). ***Supplementary Tables 2 and 3*** summarize the isomer shifts, quadrupole splittings, line widths, and fractional intensities assumed in each simulation. Each spectrum represents a single trial.

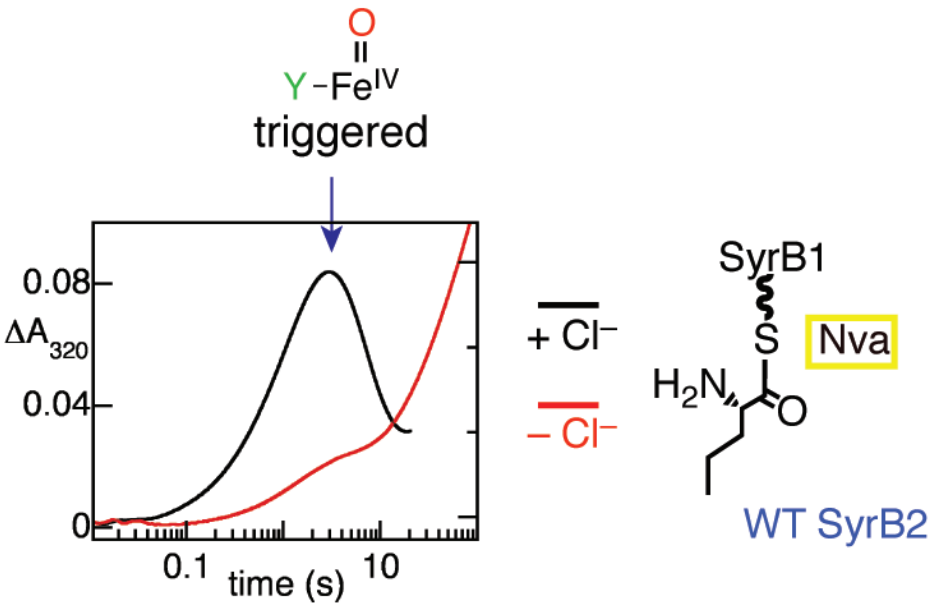

Supplementary Figure 7. Demonstration of aminoacyl-*S*-SyrB1-dependent chloride triggering in SyrB2 with the substrate previously shown to undergo primarily hydroxylation (Nva-*S*-SyrB1). Absorbance (320 nm)-versus-time traces obtained in stopped-flow experiments are analogous to those in ***Figure 4***. An O_2-saturated buffer solution was mixed with an equal volume of an O_2-free solution containing Fe(II), αKG, WT-SyrB2, and Nva-*S*-SyrB1 in the absence (***red trace***) or presence (***black trace***) of excess Cl^- (50 mM). Each trace is an average of at least three trials (stopped-flow "shots").

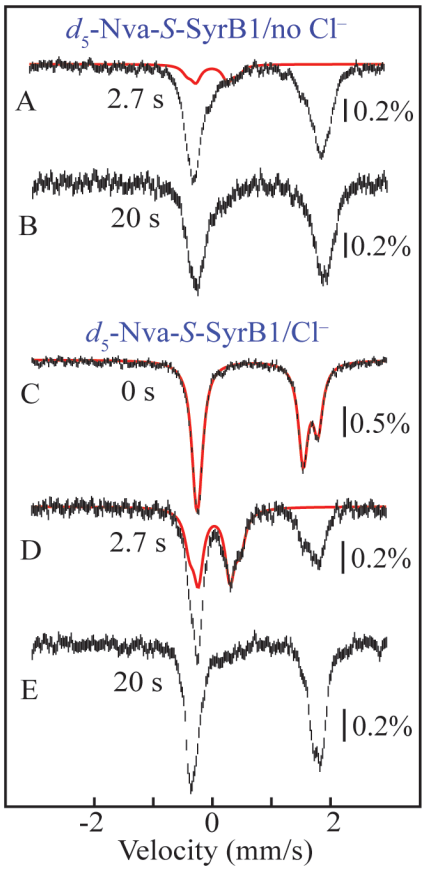

Supplementary Figure 8. Mössbauer spectra of selected samples prepared by mixing the SyrB2•Fe(II)•αKG•d_5-Nva-*S*-SyrB1 complex, in the absence or presence of added Cl^-, with O_2-saturated buffer and freeze-quenching at the indicated reaction times, which were chosen on the basis of the kinetic traces in ***Supplementary Figure 7***. Solid red lines are simulations of the summation of the Fe(II) components (in the 0-s sample) or Fe(IV) components of the Cl–Fe(IV)=O states (in the 2.7-s samples) with parameters reported in ***Supplementary Tables 2*** and ***3***. The upper limit for the intensity that can be attributed to Fe(IV) in ***a*** is ~ 20% of the corresponding intensity in ***d*** (red line). This intensity corresponds to just ~ 10% of the total iron content, or ~ 40 μM of the Fe(IV) complex, and is attributed to the Cl–Fe(IV)=O intermediate generated from contaminating Cl^-. Each spectrum represents a single trial.

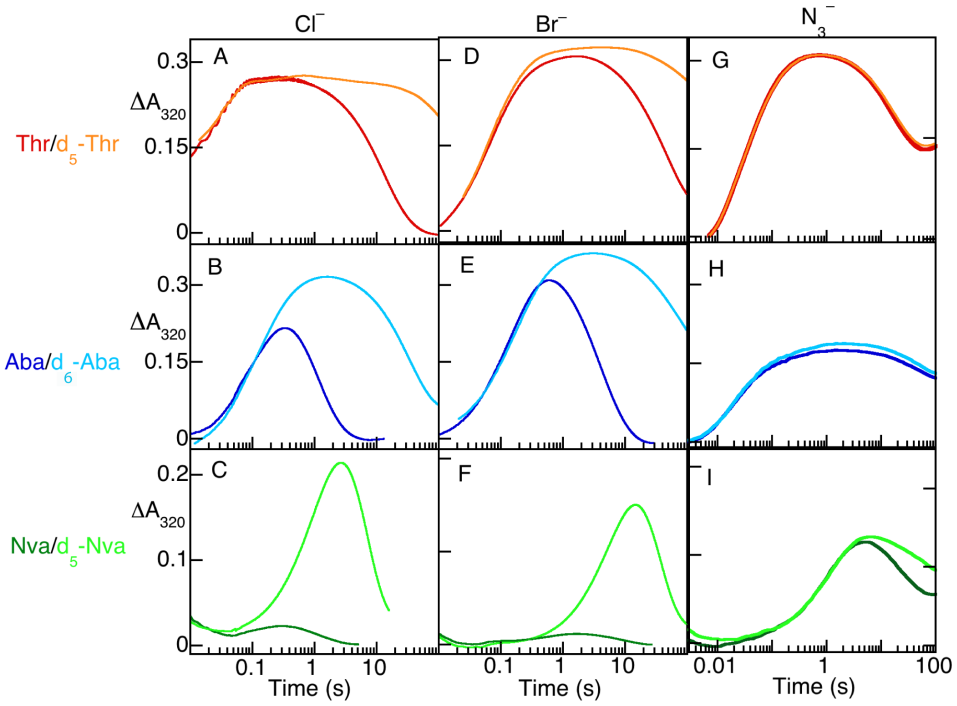

Supplementary Figure 9. ^{2}H-KIE observed on decay of chloro-, bromo- and azido-ferryl complexes formed with deuterated Thr-*S*-SyrB1, Aba-*S*-SyrB1, and Nva-*S*-SyrB1 substrates. Absorbance-versus-time traces (320 nm) obtained after O_2-saturated buffer was mixed with an equal volume of an O_2-free solution of Fe(II), SyrB2, αKG, and either Cl^- (***a-c***)[1], Br^- (***d-f***), or N_3^- (***g-i***) and either Thr-*S*-SyrB1 (*red traces*), d_5-Thr-*S*-SyrB1 (*orange traces*), Aba-*S*-SyrB1 (*dark blue traces*), d_5-Aba-*S*-SyrB1 (*light blue traces*), Nva-*S*-SyrB1 (*dark green traces*) or d_5-Nva-*S*-SyrB1 (*light green traces*). The absence of a ^{2}H-KIE in the SyrB2 reaction with N_3^- and the poorest H•-donating substrate, Thr-*S*-SyrB1, and the onset of a detectable effect upon use of the better H• donors (Aba-*S*-SyrB1 and Nva-*S*-SyrB1) suggests that at least a fraction of the intermediate decays productively via H• abstraction from the substrate. Note that the red trace in ***g*** was scaled by a factor of 1.2 to adjust for amplitude variation. All traces are averages of at least three trials (stopped-flow "shots").

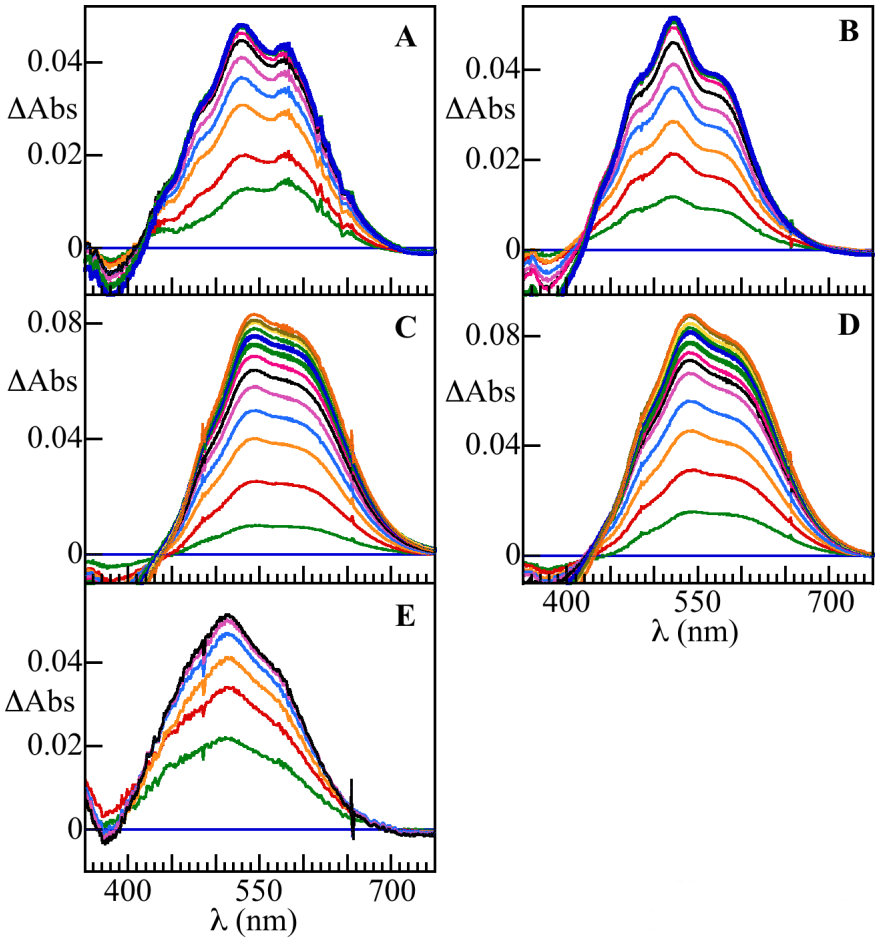

Supplementary Figure 10. Effect of anion binding to the Fe(II)•αKG•SyrB2-A118G complex on the absorption spectrum arising from the MLCT during titration of (***a***) Cl^-, (***b***) Br^-, (***c***) N_3^- (***d***) OCN^-, and (***e***) SCN^-. The method of spectral processing is summarized in ***Figure 3*****,** and the spectra are analogous to those in ***Supplementary Figure 4*** for the wild-type SyrB2 protein. Each panel represents a single trial.

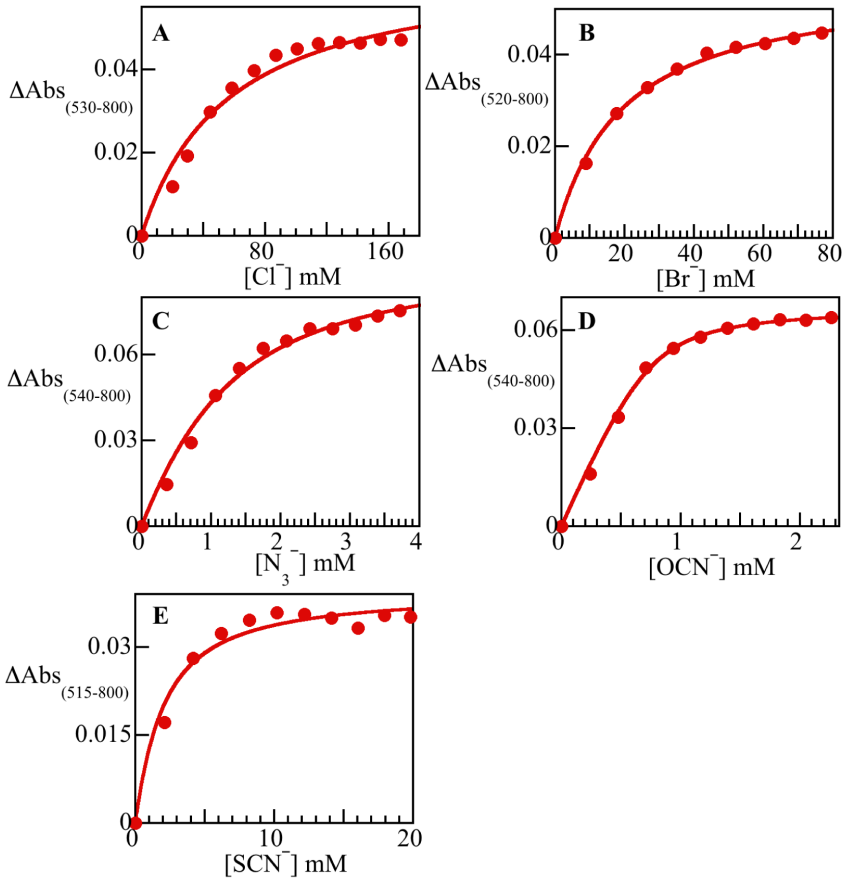

Supplementary Figure 11. Absorbance-versus-[anion] plots obtained from the difference spectra shown in ***Supplementary Figure 10***. The K_D values for the anions reported in ***Supplementary Table 1*** were determined from fitting the hyperbolic binding equation (if in the weak binding regime, as in ***a*** and ***b***) or the quadratic binding equation (if in the tight binding regime, as in ***c***, ***d***, and ***e***) to the data. Each panel represents a single trial.

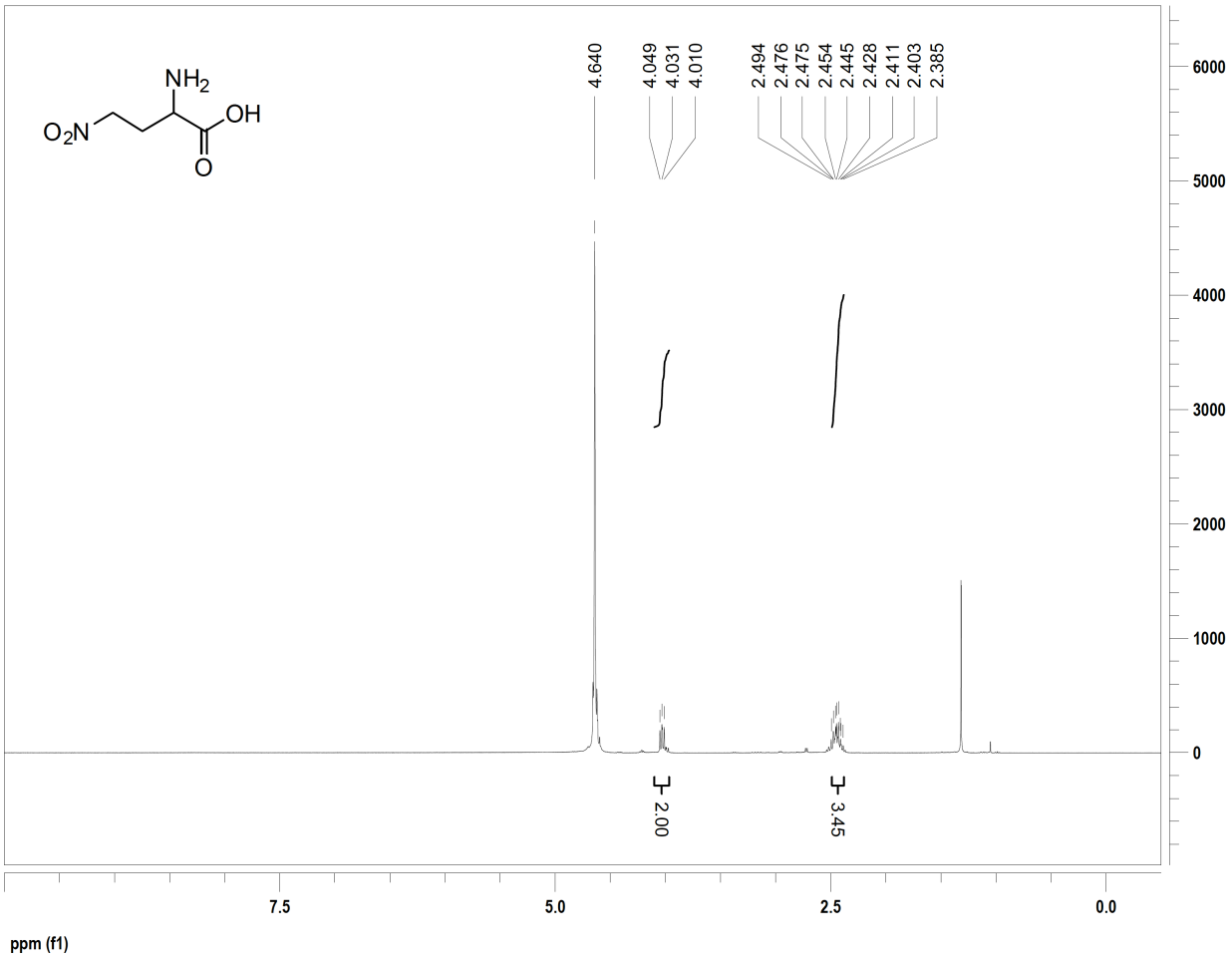

Supplementary Figure 12. ^{1}H-NMR spectrum of the synthetic 4-NO_2-Aba standard.

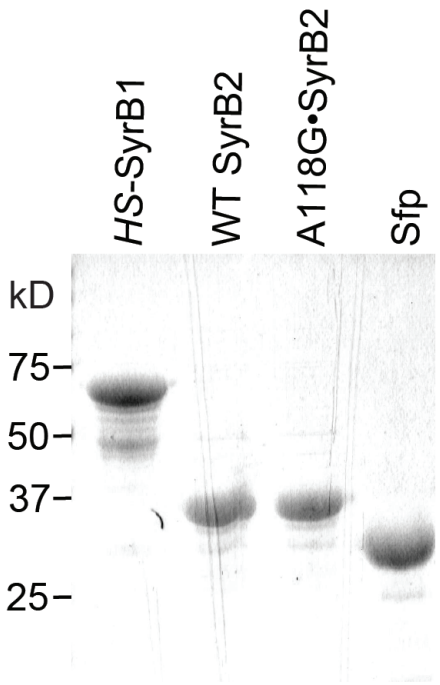

Supplementary Figure 13. Analysis of the protein preparations employed in this study by SDS-PAGE.

REFERENCES

1. Matthews, M. L. *et al.* Substrate-triggered formation and remarkable stability of the C-H bond-cleaving chloroferryl intermediate in the aliphatic halogenase, SyrB2. *Biochemistry.* **48**, 4331-4343 (2009).
2. Matthews, M. L. *et al.* Substrate positioning controls the partition between halogenation and hydroxylation in the aliphatic halogenase, SyrB2. *Proc. Natl. Acad. Sci. U. S. A.* **106**, 17723-17728 (2009).